

Advancing super resolution microscopy for quantitative in-vivo imaging of chromatin nanodomains

Clayton W. Seitz

August 12, 2024

Outline

Introduction to fluorescence nanoscopy

Contemporary approaches to fluorescence nanoscopy

Enhanced nanoscopy with deep generative models

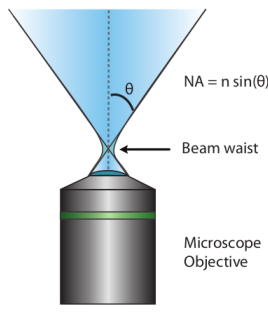
Enhanced nanoscopy with a single photon avalanche diode array

Super-resolution of nucleosome nanodomains *in-vivo*

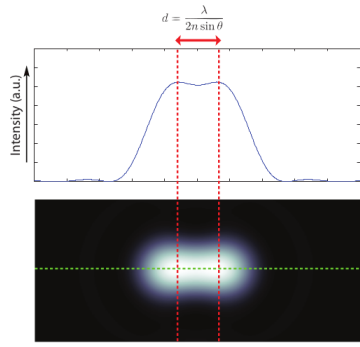
Introduction to fluorescence nanoscopy

Fluorescence microscopy and the diffraction limit

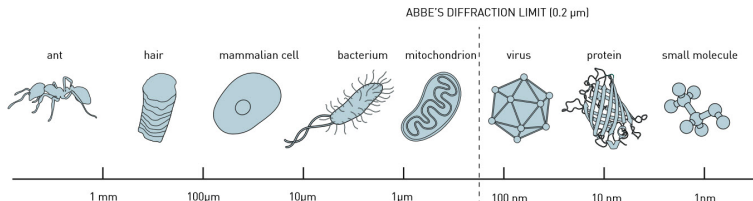
Minimal resolvable distance $d \sim \lambda$



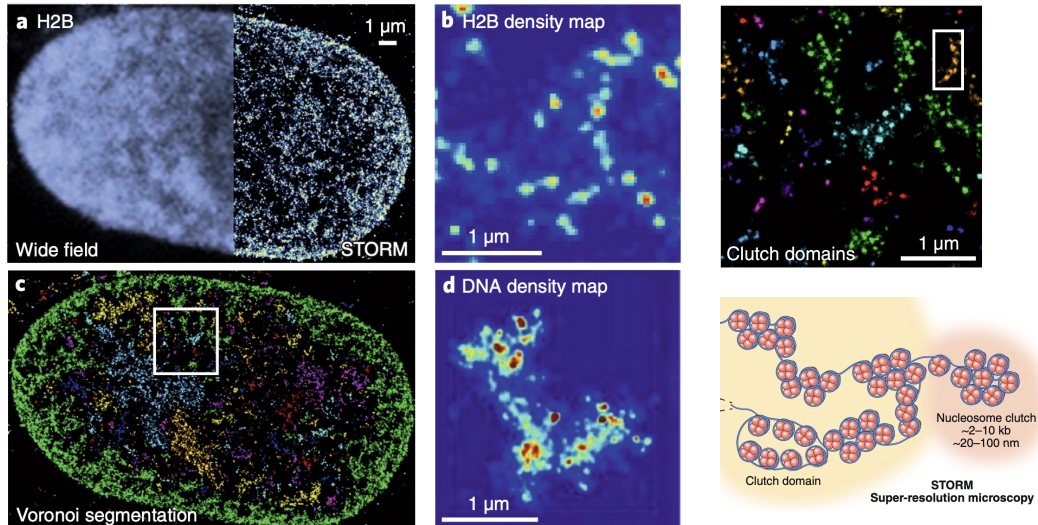
(a)



(b)

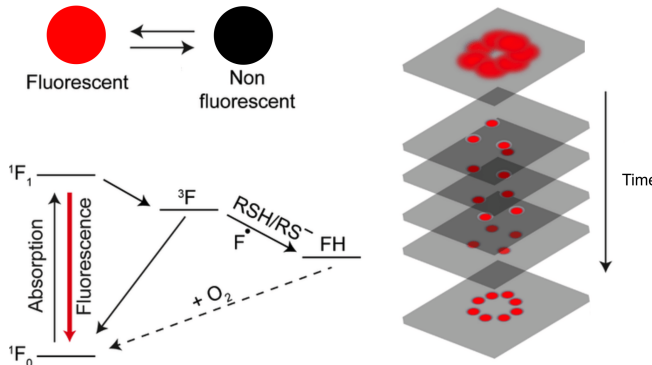


Stochastic optical reconstruction microscopy (STORM)



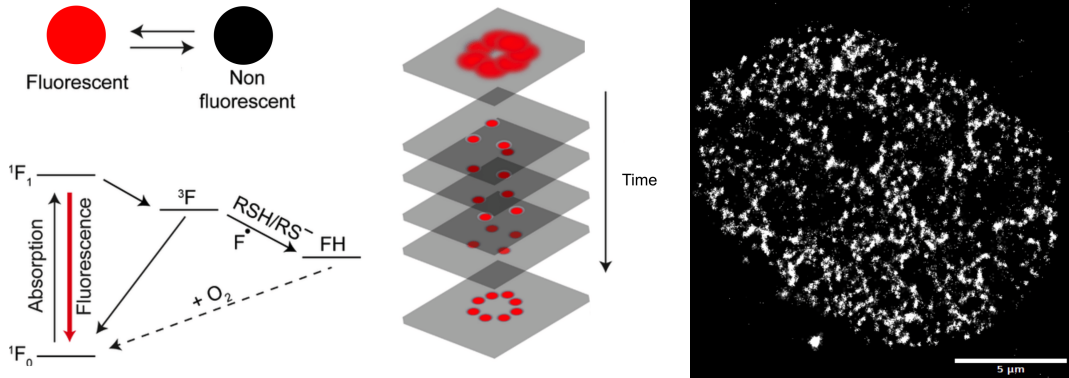
Lakadamyali, M. et al. Nature Methods **17**, (2020).

Stochastic optical reconstruction microscopy (STORM)



- ▶ STORM and similar nanoscopy techniques are diffraction-unlimited
- ▶ Photoswitching enables resolution of emitters below the diffraction limit

Stochastic optical reconstruction microscopy (STORM)



- ▶ STORM and similar nanoscopy techniques are diffraction-unlimited
- ▶ Photoswitching enables resolution of emitters below the diffraction limit

Nanoscopy by localizing isolated fluorescent emitters

Modeling the point spread function permits sub-pixel localization

$$\mu_k = i_0 \int \int O(u, v) dudv + \lambda$$

$$i_0 = g_k \eta \zeta \Delta$$

g_k – pixel gain

η – quantum efficiency

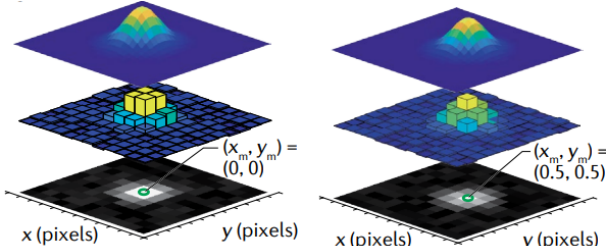
ζ – photon emission rate

Δ – exposure time

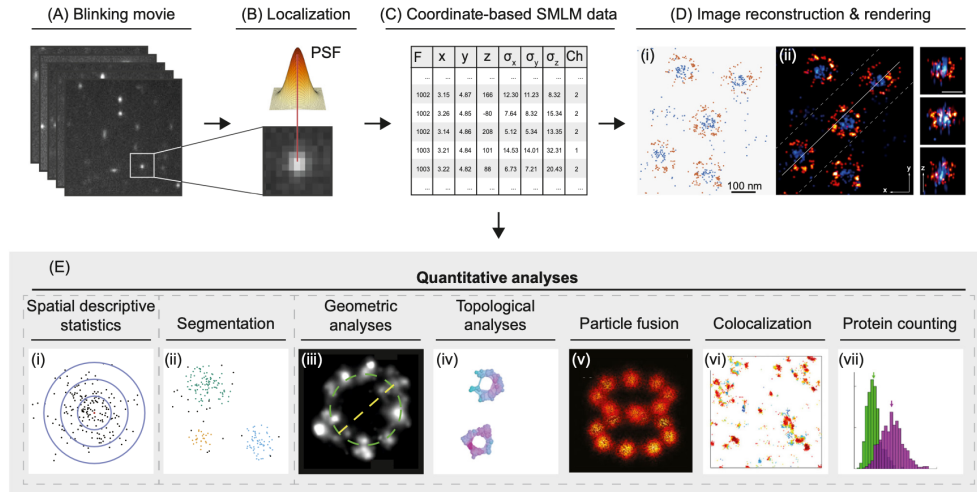
λ – background rate

Maximum likelihood localization:

$$\theta^* = \operatorname{argmax}_{\theta} \prod_k p(\mathbf{x}_k | \theta) = \operatorname{argmin}_{\theta} - \sum_k \log p(\mathbf{x}_k | \theta)$$

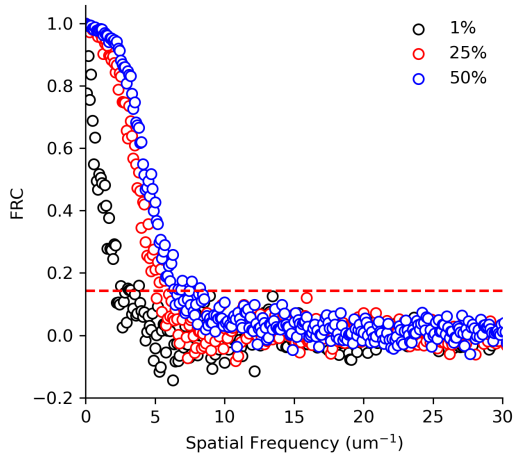
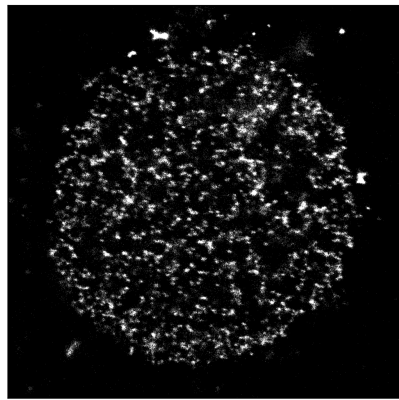


Applications of single molecule localization microscopy



Wu et al. Trends in Cell Biology. 30 (2020)

How do we define resolution in localization microscopy?



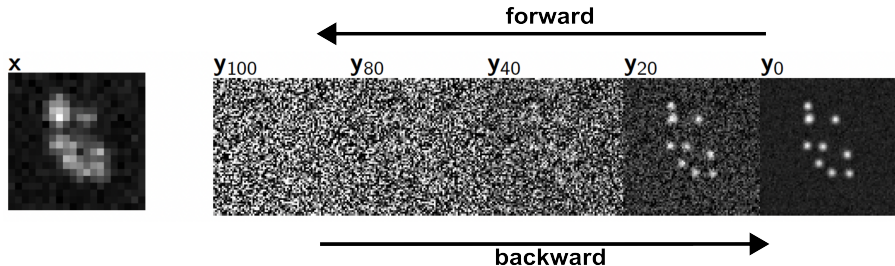
More samples → higher spatial/temporal resolution
How to relax the density limit in localization microscopy?

Contemporary approaches to fluorescence nanoscopy

Bayesian image restoration with diffusion models

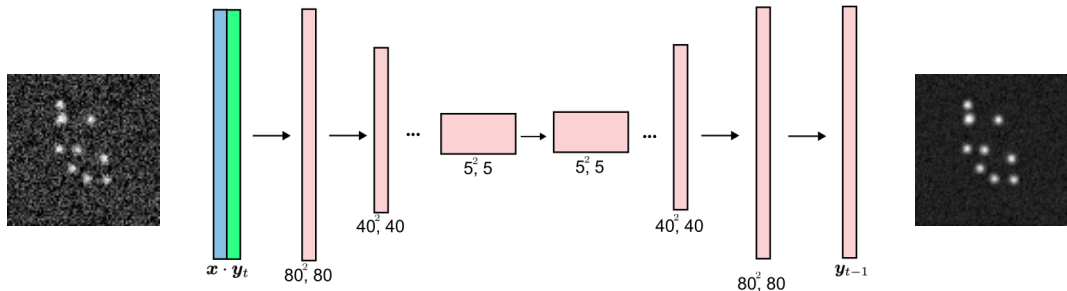
Inference of a high resolution image \mathbf{y} from low resolution \mathbf{x} is approached by modeling a distribution $p_\psi(\mathbf{y}|\mathbf{x})$ with a diffusion model

$$q(\mathbf{y}_t | \mathbf{y}_{t-1}) = \mathcal{N}\left(\sqrt{1 - \beta_t} \mathbf{y}_{t-1}, \beta_t I\right)$$



$$p_\psi(\mathbf{y}_{t-1} | \mathbf{y}_t, \mathbf{x}) = \mathcal{N}(\mu_\psi(\mathbf{y}_t, \gamma_t), \beta_t I)$$

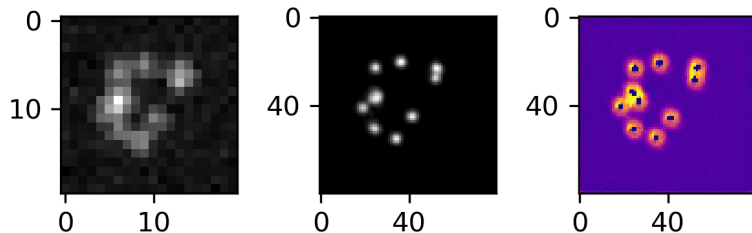
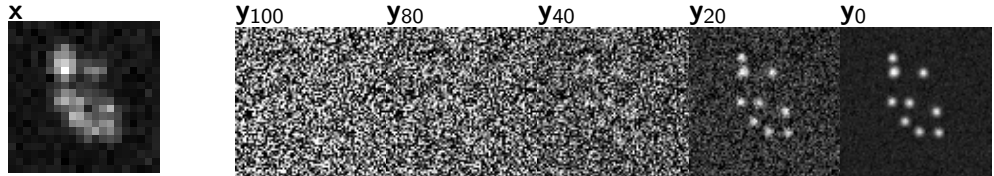
Bayesian image restoration with diffusion models



A deep neural network estimates the gradient of the reverse process

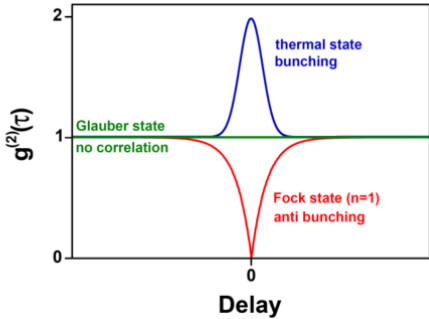
$$\mathbf{y}_{t-1} = \frac{1}{\sqrt{1 - \beta_t}} (\mathbf{y}_t + \beta_t s_\psi(\mathbf{y}_t)) + \sqrt{\beta_t} \xi \quad \xi \sim \mathcal{N}(0, I)$$

Bayesian image restoration with diffusion models



A powerful class of methods but generally lacks a physically constrained number of fluorescent emitters...

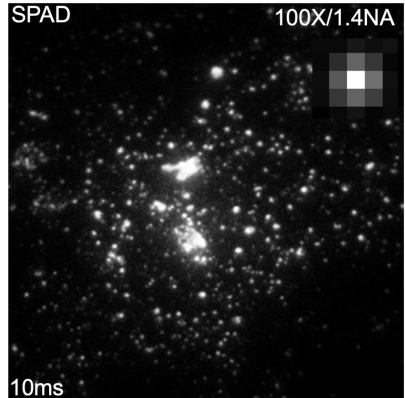
The Hanbury Brown and Twiss Effect



$$g^{(2)}(\tau) = \frac{\langle n(t)n(t + \tau) \rangle}{\langle n(t) \rangle^2}$$

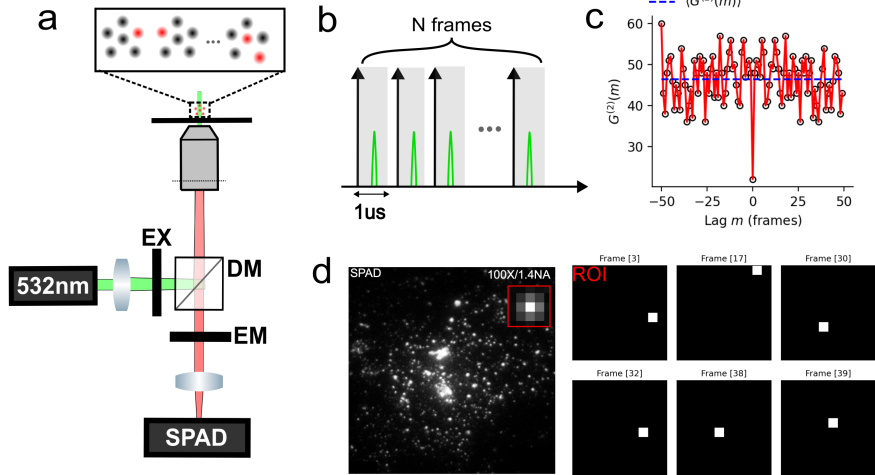
- ▶ Single photon sources (such as a fluorescent dye) exhibit antibunching
- ▶ Magnitude of $g^{(2)}(0)$ "dip" depends on the number of fluorescent emitters
- ▶ Provides a means of counting fluorescent emitters

Widefield photon counting with a SPAD array

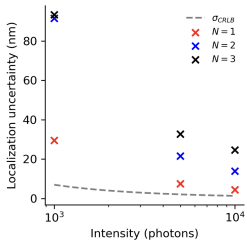
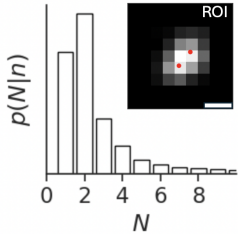
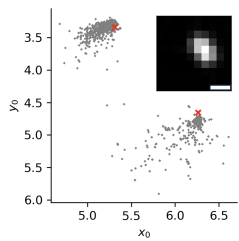
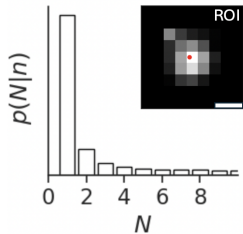


- ▶ Spatial resolution of photon counts
- ▶ Fast exposures as low as 20 nanoseconds

Imaging Qdot655 photon by photon



Constrained multi-emitter localization with photon counting

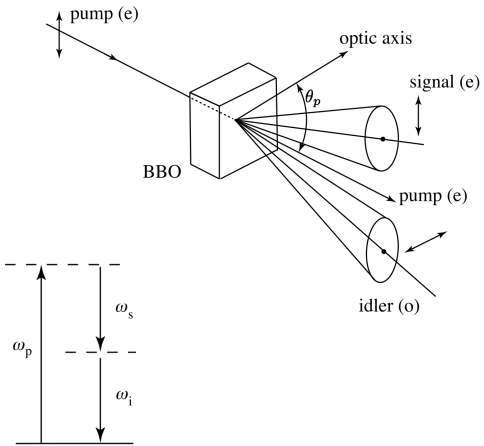
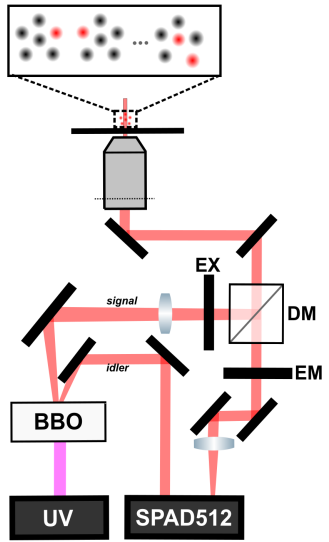


Posterior distribution on (N, ζ) :

$$p(N, \zeta|n) \propto p(n|N, \zeta)p(\zeta)$$

- ▶ MAP estimation on N
- ▶ Parameterization of multi-emitter fitting
- ▶ Approaches σ_{CRLB} for $N = 1$

Heralding single photons with parametric downconversion



Heralding single photons with parametric downconversion



ROI 1

ROI 2

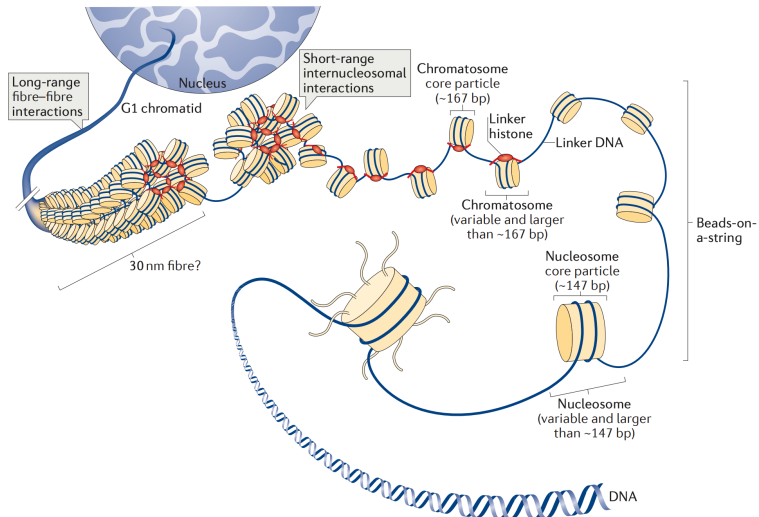
AND-image

$\left(\begin{array}{l} \text{rotated by} \\ \text{angle of } \pi \end{array} \right)$

- ▶ Detection of dark counts or background counts
- ▶ Noise free nanoscopy

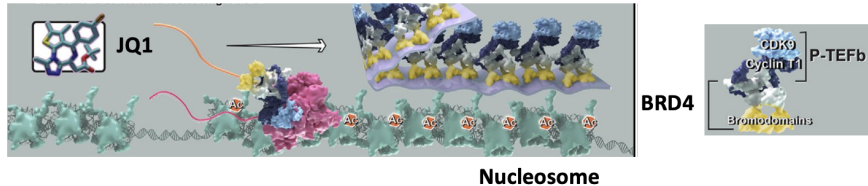
Super-resolution of nucleosome nanodomains *in-vivo*

Hierarchical structure of chromatin

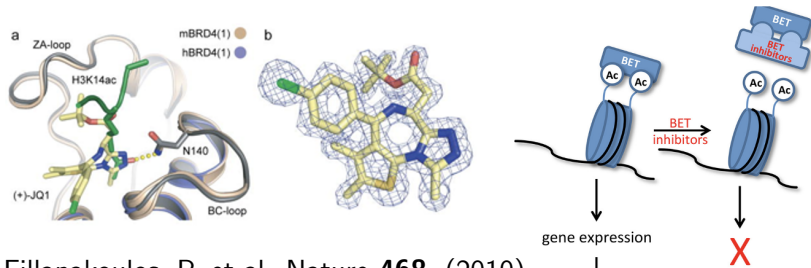


Fyodorov, D. et al. Nat Rev Mol Cell Biol **19**, (2018).

Bromodomain protein 4 (BRD4) binds acetylated chromatin

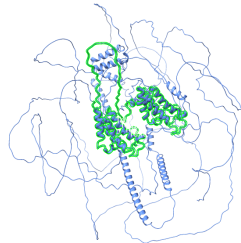
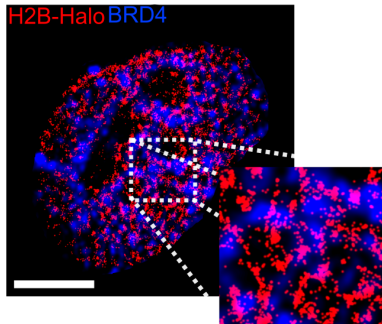


Zheng, B. et al. Molecular Cell **16**, (2023).



Fillapakoulos, P. et al. Nature **468**, (2010).

Bromodomain protein 4 (BRD4) binds acetylated chromatin

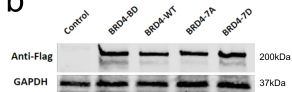


BRD4 phosphorylation state is necessary for maintenance of chromatin structure

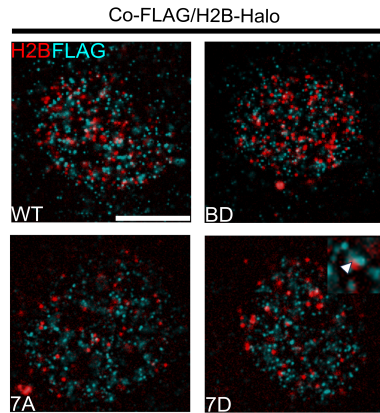
a



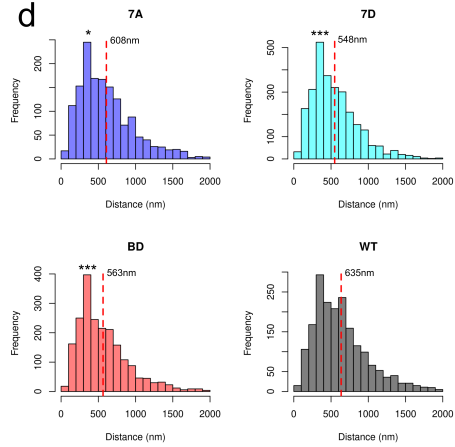
b



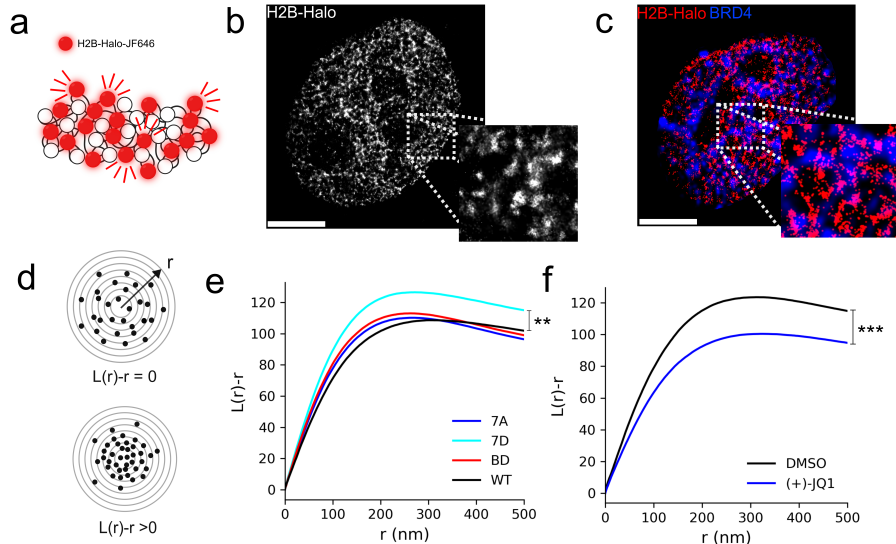
c



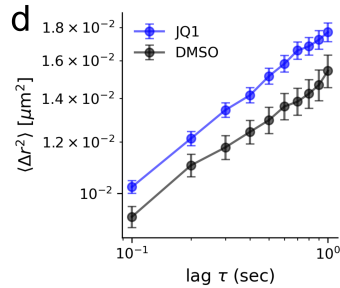
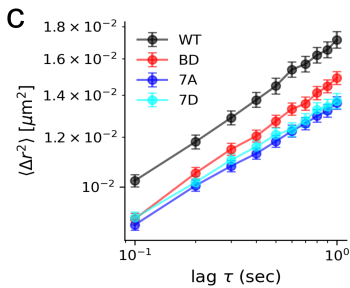
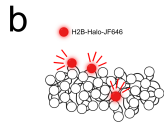
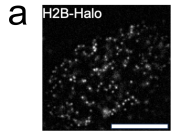
d



BRD4 phosphorylation state is necessary for maintenance of chromatin structure

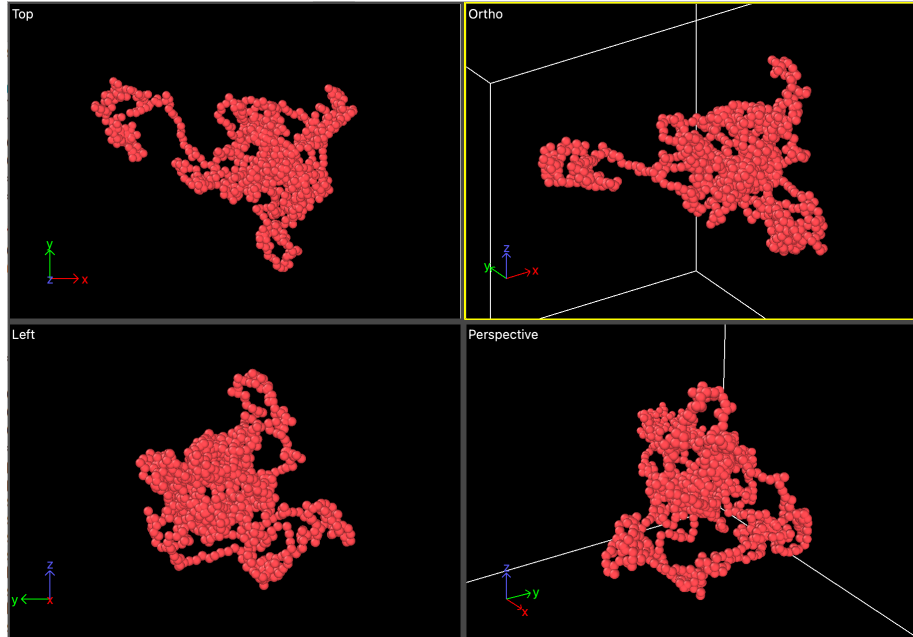


Multivalent chromatin binding reduces chromatin mobility



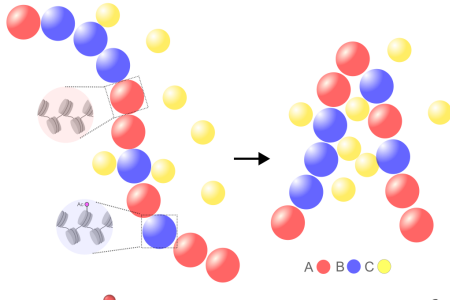
Experiment: $D_{W\tau} - D_{7D} \approx 10^{-3} \mu\text{m}^2/\text{s}, \gamma = 10^{-6}$

Coarse grained molecular dynamics of chromatin at 310K

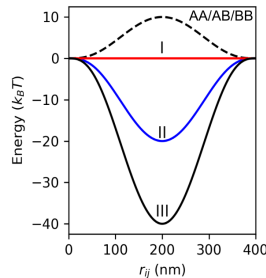


Coarse grained molecular dynamics of chromatin binders at 310K

a



b

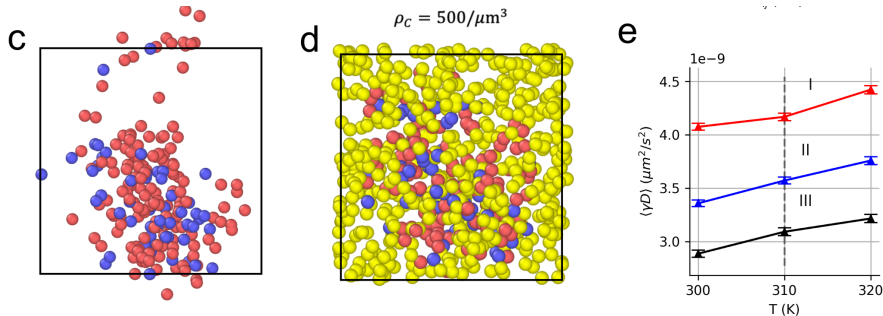


100kb chromatin chains interact with binders via the potential

$$U_{ij} = \epsilon \left(1 - \left(\frac{|r_{ij}|}{R_0} \right)^2 \right)^3$$

- ▶ A (B) type particles represent unacetylated (acetylated) chromatin beads
- ▶ BRD4-like C particles bind B type particles with variable energies

Multivalent chromatin binding reduces chromatin mobility



Integrate Brownian dynamics: $\dot{r} = \gamma^{-1} \nabla U + \sqrt{2k_B T} \gamma^{-1/2} \xi$ $\gamma = 10^{-6}$

Stochastic forcing is a delta-correlated white-noise
 $\xi \sim \mathcal{N}(0, 1)$, $\langle \xi(t) \xi(t + \tau) \rangle = \delta(\tau)$